molecules versus tetrahedrally coordinated monoatomic univalent ions and deduced that the nature of the solvent isotope effect is due to changes in librational frequencies of water induced by the presence of ions. Only F^- led to an increase in librational frequency with all other anions yielding decreases. These authors have thus interpreted the fluoride system as unique with solution in D_2O favored over H_2O because of the greater spacing of librational energy levels relative to pure water.

Conclusion

The equilibrium constants for isotope exchange reactions between gaseous water molecules and the four gaseous ions L_3O^+, $L_5O_2^+$, $(L_2O)F^-$, and $(L_2O)Cl^-$ have been determined from ion cyclotron resonance equilibrium techniques.

The value for isotopic fractionation factor of gaseous L_3O^+ is found to be essentially identical with that observed for isolated hydronium ion in acetonitrile. These result infers that hydrogen bonding from hydronium ion to acetonitrile in solution phase has a negligible effect on the fractionation factor. The results for L_3O^+ and $L_5O_2^+$ also fully support the results and conclusions drawn from experiments for these ions in aqueous solution. Specifically the increase in fractionation factor from gaseous hydronium ion to fully hydrated hydronium ion in solution is due to the extensive hydrogen bonding network present in solution. This is evident from the greater gas-phase fractionation factor of $L_5O_2^+$ relative to L_3O^+.

Hydrogen bonding of L_3O^+, F^-, and Cl^- to L_2O lowers the fractionation factors relative to that observed for gaseous H_2O. The effect of F^- on the fractionation factor is opposite to that expected on the basis of F^- behavior in aqueous solution and on the basis of relative F^- and Cl^- solution phase behavior. This is apparently associated with the dominance of zero-point energy effects on solution phase isotope effects, whereas in the gas phase for such small ions rotational contributions to the isotope effect become very important.

The experimental data consistently reveal that the mixed H/D species DOH_2^+, D_2OH^+, $H_3D_2O_2^+$, $(HOD)F^-$, and $(HOD)Cl^-$ are considerably less abundant than would be predicted on the basis of the "rule of the geometric mean" and the abundance of the fully deuteriated and protonated species. This is again almost certainly due to the combined importance of the MMI, EXC, and ZPE contributions to the overall isotope effects for such small ions.

The continued investigation of isotope effects for gaseous ions will hopefully provide further insights into the origin of such affects and lend credibility to mechanistic deductions based on isotope effects for solution phase ions. We would also suggest that the extent to which calculated vibrational frequencies used in statistical thermodynamic calculations of isotope effects are able to reproduce experimentally measured values will provide a rigorous measure of the level of the accuracy of vibrational frequencies. In particular temperature dependent studies are planned to obtain a measure of the ZPE component of some isotope effects.

Further, should spectroscopic investigations of the interstellar medium ultimately be successful in detecting H_3O^+, H_2OD^+, HOD_2^+, and D_3O^+ as a means of probing the existence of water the equilibra examined here will allow inference of the relative amounts of H_2O, HOD, and D_2O to be made.[32,33]

Acknowledgment. Financial support of this work by the National Sciences and Engineering Research Council of Canada (N.S.E.R.C.) and the Petroleum Research Fund of the American Chemical Society (ACS-PRF) is gratefully acknowledged. J. Fisher and C. Allison are thanked for assistance in calculations of moments of inertia.

Registry No. H^+, 12586-59-3; H_3O^+, 13968-08-6; F^-, 16984-48-8; Cl^-, 16887-00-6; D_2, 7782-39-0.

---

(32) Smith, D.; Adams, N. *Int. Rev. Phys. Chem.* **1981**, *1*, 271.

(33) Smith, D. *Philos Trans. Roy. Soc.* **1981**, *303*, 535.

Synchrotron Radiation Selected *s*-Tetrazine Ion Chemistry

I. Nenner,*[†] O. Dutuit,[‡] M. Richard-Viard,[§] P. Morin,[†] and A. H. Zewail[∥,⊥]

Contribution from LURE, Laboratoire mixte CNRS, CEA et MEN, Université de Paris Sud, Bât. 209 C, 91405 Orsay, Cedex, France. *Received June 19, 1987*

Abstract: With use of synchrotron radiation (9–22 eV) the photon-selected chemistry of *s*-tetrazine ion is reported. Dissociation intermediates and products are investigated by the threshold photoelectron–photoion coincidence technique. On the basis of breakdown curves and thermodynamics, the loss of N_2 is found to be associated with the $C_2N_2H_2^+$ ion with an activation energy of 0.96 eV. Smaller fragment ions such as $HCNH^+$ and HCN^+ originate from single bond breaking of the $C_2N_2H_2^+$ primary fragment ion rather than the dissociation of the parent ion.

I. Introduction

The fragmentation of the *s*-tetrazine molecule ($C_2N_4H_2$) into one N_2 and two HCN molecules[1,2] after its photoexcitation to the lowest singlet states has raised several questions.[3,4] One question concerns the identification of the "active" excited state which can be reached with a single photon in the visible or near-UV spectrum. Another deals with the dynamics of the photodissociation process itself, which involves either a direct triple fragmentation through a specific transition state or a sequential dissociation.[3-5] The consensus appears to be in favor of a simultaneous triple fragmentation.[3-5] However, it is difficult to prove such a mechanism.

In this paper we report studies of the fragmentation of *s*-tetrazine ion, photoselected by synchrotron radiation in the energy

---

[†] CEA-IRDI/DESICP-Département de Physico-Chimie, 91191 Gif sur Yvette, Cedex, France.

[‡] LPCR, U.A. 75, Université Paris Sud, Bât. 350, 91405 Orsay, Cedex, France.

[§] LCAM, U.A. 281, Université Paris Sud, Bât. 351, 91405 Orsay, Cedex, France.

[∥] A. A. Noyes Laboratory of Chemical Physics, California Institute of Technology, Pasadena, CA 91125. Contribution No. 7606.

[⊥] John Simon Guggenheim Foundation Fellow.

(1) Hochstrasser, R. M.; King, D. S. *J. Am. Chem. Soc.* **1975**, *97*, 4760.

(2) Coulder, D.; Dows, D.; Reisler, H.; Wittig, C. *Chem. Phys.* **1978**, *32*, 429.

(3) King, D. S.; Denny, C. T.; Hochstrasser, R. M.; Smith, A. B. *J. Am. Chem. Soc.* **1977**, *99*, 271.

(4) Glownia, J. H.; Riley, S. J. *Chem. Phys. Lett.* **1980**, *71*, 429.

(5) Scheiner, A. C.; Scuseria, G. E.; Schaeffer, H. F., III *J. Am. Chem. Soc.* **1986**, *108*, 8160.

0002-7863/88/1510-1093$01.50/0

range 9–22 eV (1 eV $\approx$ 96 kJ mol^{-1}). With use of photoelectron–photoion coincidence techniques, the ion intermediates and fragments are studied and related to the dynamics of dissociation of the ion and neutral. Studies of the ion fragmentation offer some advantages.

First, the photoelectron–photoion coincidence method allows for measurement of fragmentation branching ratios, translational energy released in the dissociation reaction, and dissociation rate (time scale of nanosecond or longer) of energy selected ions. These methods, reviewed by Baer,[6] can be combined either with fixed photon energy sources (the ion energy is selected by the electron energy) or with tunable photon energy sources (only zero kinetic energy electrons are detected); the photon energy directly provides the energy selection of the ion. Here, we use the latter method, known as threshold photoelectron–photoion coincidence (TPEPICO), in association with synchrotron radiation in the vacuum UV (9–22 eV).

Second, the fragmentation of the parent ion can be useful in understanding the dissociation of the neutral. The ground electronic state of $C_2N_4H_2^+$ is known to result from the ejection of a nonbonding electron ($2b_{1g}$). This is based on photoelectron spectroscopic measurements[7,8] and theoretical calculations.[9] The thermodynamic dissociation limit corresponding to the loss of N_2 lies below the parent ion ground state. This situation is similar to that of the neutral molecule. Consequently, the stability and the fragmentation of the ions near threshold may resemble those of the neutral species.

The results of the work reported here indicate several points regarding the fragmentation of the ion. The loss of N_2 from the tetrazine ion (primarily) involves the formation of two fragments, rather than the three fragments suggested for the neutral molecule. Furthermore, fragments found in the 1–3-eV region above threshold originate from sequential events rather than direct dissociation of the parent ion into three fragments. The possible structures of fragmentations, which are of current astrophysical interest[10,11] and are related to the problem of HCN oligomerization,[12] are discussed.

II. Experimental Section

The detailed description of our experimental setup can be found in ref 13 and 14. Briefly, synchrotron radiation from the ACO storage ring at Orsay is dispersed by a 1-m normal incidence monochromator in the 9–25 eV photon energy range. When used below 11.8 eV (above 1050 Å), the photon beam is filtered by a LiF window in order to reject higher order contributions. The monochromatic radiation is then refocused in the center of the new double time of flight spectrometer.[15] Electrons and ions are extracted in opposite directions, perpendicularly to both the light beam and gas jet. The threshold electrons are energy selected[13-15] by angular and time-of-flight discrimination, thus taking advantage of the pulsed character of synchrotron radiation. The internal energy of the parent ions associated with such threshold electrons is uniquely selected by the incident photon energy. Parent and fragment ions are extracted in coincidence with threshold electrons by applying a pulsed voltage (30–100 V/cm) on the first acceleration stage of the spectrometer. The voltages applied on the first and the second acceleration stages as well as the drift region are optimized to achieve an improved mass resolution compared to previous setups.[13,14] The time-of-flight broadening provides the kinetic energy released in the dissociation.

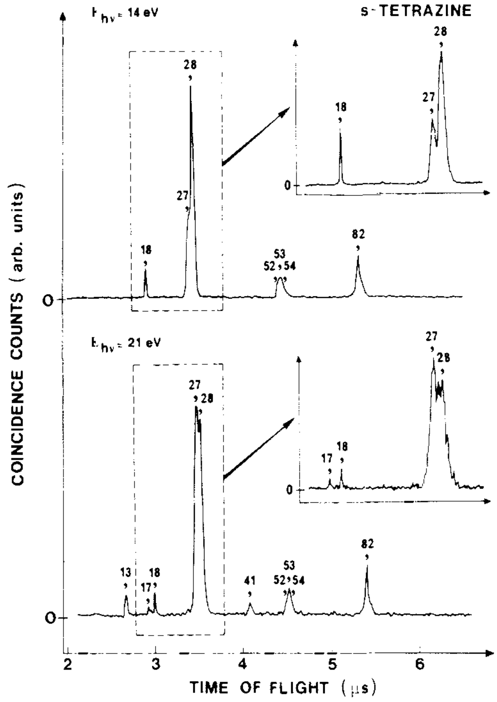

Figure 1. Pseudo mass spectra of tetrazine for not-selected electrons and ions, with 200 V/cm extraction field: (a) at 14 eV photon energy, (b) at 21 eV photon energy, detailed spectra are shown in inserts.

s-Tetrazine was synthesized with the method described by Spencer et al.[16] The last part of this process, which is very inefficient, was performed under vacuum. The carboxylic acid was mixed with dry sand and placed in a glass bulb. Decarboxylation was achieved by heating the bulb in an oil bath, and *s*-tetrazine crystals were collected in a cooled trap. The purity was checked by infrared and visible spectrometry.[17]

III. Results

A. "Pseudo" Mass Spectra. Mass spectra were obtained by measuring the time-of-flight of ions with respect to the electron signal, without selecting them in time. They are considered as pseudo mass spectra because our strong geometrical discrimination against energetic electrons reduces the detection of ions associated with energetic electrons ($E \geqslant 1$ eV) to a few percent and the fragmentation branching ratio is somewhat different. Nevertheless, these pseudo mass spectra give an overview on the integrated fragmentation pattern of the parent ion produced from threshold up to the nominal energy and its changes with incident photon energy.

Figure 1a shows a typical pseudo mass spectrum of *s*-tetrazine obtained at 14 eV photon energy. We observe four major peaks. The *m/z* 82 peak is the parent ion $C_2N_4H_2^+$ and represents $\sim$12% of the total. The *m/z* 54 peak corresponds to the formula $C_2N_2H_2^+$ (or CN_3^+) and represents $\sim$11% of the total. The most prominent fragments are *m/z* 27 and 28 which correspond respectively to HCN^+ and $HCNH^+$ (or N_2^+). They represent $\sim$23% and 54% of the total, as extracted from the enlarged spectrum (shown in the insert of Figure 1a). The *m/z* 18 peak originates from water impurity. When the photon energy is increased to 21 eV, the fragmentation increases as seen in Figure 1b. The parent ion represents only 8.5% of the total. While the relative abundance of the 54 peak decreases to 8.5%, the importance of the *m/z* 27 peak overcomes the 28 one. The analysis of the detailed spectrum (see insert) shows that the *m/z* 27 and 28 peaks are no longer resolved because both peaks widened by large kinetic energy releases in the dissociation process. Nevertheless, it is interesting to note that the contribution of *m/z* 27

---

(6) Baer, T. In *Gas Phase Ion Chemistry*; Bowers, M. T., Ed.; Academic: New York, 1979; Chapter 5; pp 153–196.

(7) Gleiter, R.; Heilbronner, E.; Hornung, V. *Helv. Chim. Acta* **1972**, *55*, 255.

(8) Fridh, C.; Åsbrink, L.; Jonsson, B. O.; Lindholm, E. *Int. J. Mass Spectrom. Ion Phys.* **1972**, *9*, 485.

(9) Von Niessen, W.; Kraimer, W. P.; Dierksen, G. H. F. *Chem. Phys.* **1979**, *41*, 113 and references therein.

(10) Haese, N. N.; Woods, R. C. *Chem. Phys. Lett.* **1979**, *61*, 396.

(11) *Molecular Astrophysics*, Diercksen, G. H. F., Huebner, W. F., Langhoff, P. W., Eds.; Reidel: Dordrecht, 1985.

(12) Clemmons, J. H.; Jasien, P. G.; Dykstra, C. E. *Mol. Phys.* **1983**, *48*, 631. Ferri, J. P.; Joshi, P. C.; Edelson, E. H.; Lawlers, J. G. *J. Mol. Evol.* **1978**, *11*, 293. Ferris, J. P.; Hagan, W. J., Jr. *Tetrahedron* **1984**, *40*, 1093

(13) Nenner, I.; Guyon, P. M.; Baer, T.; Govers, T. R. *J. Chem. Phys.* **1980**, *72*, 6587.

(14) Richard-Viard, M.; Dutuit, O.; Lavollée, M.; Govers, T.; Guyon, P. M.; Durup, J. *J. Chem. Phys.* **1985**, *82*, 4054.

(15) Richard-Viard, M. Thèse de doctorat d'Etat, Université de Paris Sud, Orsay, 1987.

(16) Spencer, G. H., Jr.; Cross, P. C.; Wiberg, K. B. *J. Chem. Phys.* **1961**, *35*, 1925.

(17) Baudin, C.; Ruaudel, A., private communication.

Table I. Relative Abundance of Fragments in *s*-Tetrazine Ion Dissociation

photon energy (eV) or internal energy	27 (*m/z*)	28 (*m/z*)	30 (*m/z*)	41 (*m/z*)	46 (*m/z*)	52, 53, 54 (*m/z*)	69 (*m/z*)	82 (*m/z*)
9.5	-	-	-	-	-	-	-	100
9.7	-	-	-	-	-	-	-	100
9.77	-	-	-	-	-	-	-	100
10.19	-	-	-	-	-	3	-	97
10.29	-	<2	-	-	-	44	-	37
10.39	-	<4	-	-	-	90	-	6
10.49	-	6	-	-	-	80	-	4
11.0	-	64	-	-	-	25	8	2
11.18	-	62	2	<1	-	5, 8, 6	15	2
11.7	~5	77	-	-	6	9	<1	1

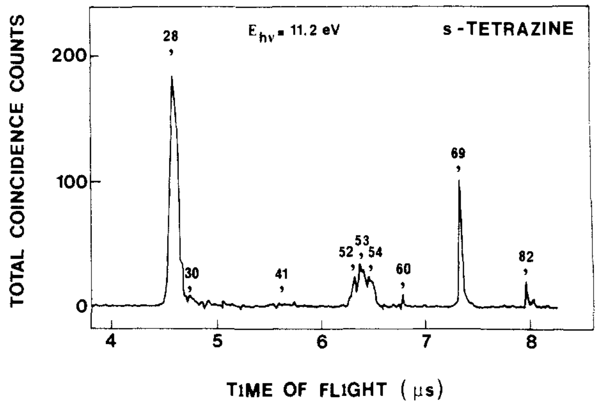

Figure 2. Typical *threshold* photoelectron-photoion coincidence spectrum of *s*-tetrazine measured at 11.2 eV photon energy and 60 V/cm extraction field.

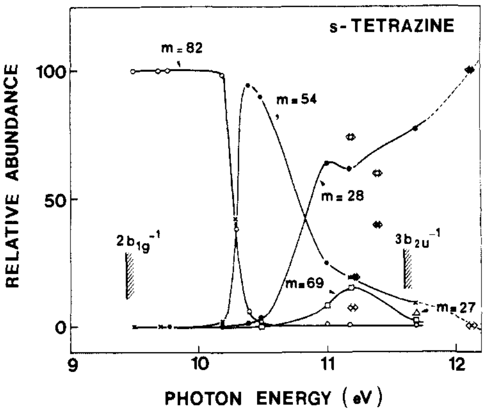

Figure 3. Breakdown curves of *s*-tetrazine ion near threshold. Symbols in brackets are from charge exchange experiments in ref 8. Energies of the ground state $(2b_{1g})^{-1}$ of tetrazine ion and first excited state $(3b_{2u})^{-1}$ are indicated.

and 28 over the total stays constant (~77%). New fragments appear (*m/z* 13 and 41) and are likely due to CH^+ and HCN_2^+. The water signal is now split into *m/z* 18 and 17; H_2O^+ is known to partially dissociate into OH^+ at 21 eV internal energy.[18]

The above (first reported) photon impact mass spectra depart significantly from the 76 eV electron impact mass spectrum, obtained by Weininger and Thornton.[19] The main fragments (*m/z* 27, 28, 53–54) as well as *m/z* 41 are found with comparable intensity with 21 eV photon or 76 eV electron impact. In contrast, we do not observe the *m/z* 26 or 29 fragments that are found by electron impact with 3.99% and 1.06% intensity, respectively. We do observe, however, the *m/z* 13 fragment that was not reported before. In fact, it is not possible to compare directly these mass spectra for several reasons: (1) electron and photon impact do not produce the same electronic states; (ii) the energy of the impinging particle (electron or photon) has generally a strong effect on the fragmentation branching ratio, and (iii) in our experiment, fragment ions associated with energetic electrons are discriminated against.

B. Fragmentation of Energy-Selected Ions. In Figure 2, we show a typical TPEPICO spectrum of *s*-tetrazine obtained at 11.2 eV photon energy. It is striking to observe more fragments than conventional mass spectra, obtained at high photon energy, would suggest. In particular, we observe fragments of *m/z* 30, 60, and 69 that were not observed in conventional mass spectra. We also notice that the 28 peak is found to be wider in Figure 2 than fragments with higher masses. The broadening is found to be 110 ns, which corresponds to 300 ± 70 meV for the kinetic energy released in the dissociation.

Similar measurements were performed at other selected photon energies from the ionization threshold (~9.24 eV) up to 11.7 eV, which is the maximum photon energy transmitted by the LiF window. We thus obtain the fragmentation branching ratios, or breakdown curves, reported in Table I and Figure 3. Such fragmentation branching ratios previously reported by Fridh et al.[8] with a charge exchange method are also reported in Figure 3. At 11.2 and 11.4 eV, there is a large discrepancy, whereas the extrapolation of our data to 12.13 eV seems to fit much better with the data of ref 8. This shows that only the Xe^+ charge exchange at 12.13 eV is resonant in energy, i.e., the energy transferred to the *s*-tetrazine is equal to the IP differences. At 11.2 and 11.4 eV, which correspond to charge transfer reactions from COS^+ and $C_2H_2^+$, respectively, as much as 1 eV of the available energy evidently was transformed into internal excitation of COS and C_2H_2, and not into internal excitation of the *s*-tetrazine ion.

As shown in Figure 3, the parent ion is found to be stable from threshold to 10.2 eV. At this energy, the parent ion dissociates into a unique fragment with *m/z* 54, which is either due to $C_2N_2H_2^+$ or CN_3^+, as discussed below. At higher energy, i.e., 11.2 eV, we also observe peaks with *m/z* 53 and 52 readily assigned to $C_2N_2H^+$ and $C_2N_2^+$. Nevertheless, the reaction leading to *m/z* 54 seems almost complete within 0.2 eV, which is our overall energy resolution. This behavior is as expected for a reaction that is fast. This situation contrasts that of the *m/z* 28 fragment which rises more slowly with increasing internal energy. The 69 fragment, which can only be assigned to CN_4H^+ (loss of CH), seems to be present solely within a narrow photon energy range around 11.2 eV. Although this *m/z* 69 fragment has been observed in two different tetrazine samples we cannot rule out completely that it is due to an impurity. The fact that this fragment is negligible in conventional (or pseudo) mass spectra is not surprising. This is because such a mass spectrum basically represents the result of the convolution of the integral of breakdown curves, from the first ionization threshold up to the nominal ionizing energy, with the internal energy distribution of the parent ion given approximately by the photoelectron spectrum. Since the *m/z* 69 ion appears in the Franck–Condon gap between the ground and first excited states, its contribution of the total mass spectrum could well be negligibly small. It is also not surprising that this ion was missed by the charge exchange experiments since, as already pointed out, the energy deposited to the tetrazine ion at 11.2 eV is in fact considerably less than the nominal energy of OCS^+ or $C_2H_2^+$.

---

(18) Eland, J. H. D. *Chem. Phys.* **1975**, *11*, 41.
(19) Weininger, S. J.; Thornton, E. R. *J. Am. Chem. Soc.* **1967**, *89*, 2050.

Table II. Thermochemistry of *s*-Tetrazine Ion Dissociation

species	m/z	$\Delta H_f°_{298}$, kJ/mol	appearance energy, (eV)	precursor	neutral fragment
$C_2H_4H_2$		427.8[a]	–	–	–
$C_2N_4H_2^+$	82	–	9.24[b]	–	–
$C_2N_2H_2^+$	54	–	10.20[c]	$C_2N_4H_2^+$	N_2
$C_2N_2H^+$	53	–	–	$C_2N_2H_2^+$	H
$C_2N_2^+$	52	1597[e]	–	$C_2N_2H_2^+$ (or $C_2N_2H^+$)	H_2 (or H)
$HCNH^+$	28	941[d]	10.50[c]	$C_2N_2H_2^+$	CN
CN_4H^+	69	–	11.00[c]	$C_2N_4H_2^+$	CH
$N_2H_2^+$	30	–	<11.20[c]		
HCN^+	27	1447[e]	11.40[c]	$HCNH^+$	
$N_2^+(X^2\Sigma_g^+)$	28	1503.3[e]		$C_2N_4H_2^+$	2HCN (or $C_2N_2H_2$)
HCN_2^+	41	–	<21 eV[c]	$C_2N_2H_2^+$	CH
CH^+	13	1619[e]	<21 eV[c]		

[a] Reference 20. [b] Reference 8. [c] This work. [d] Reference 21. [e] Reference 22.

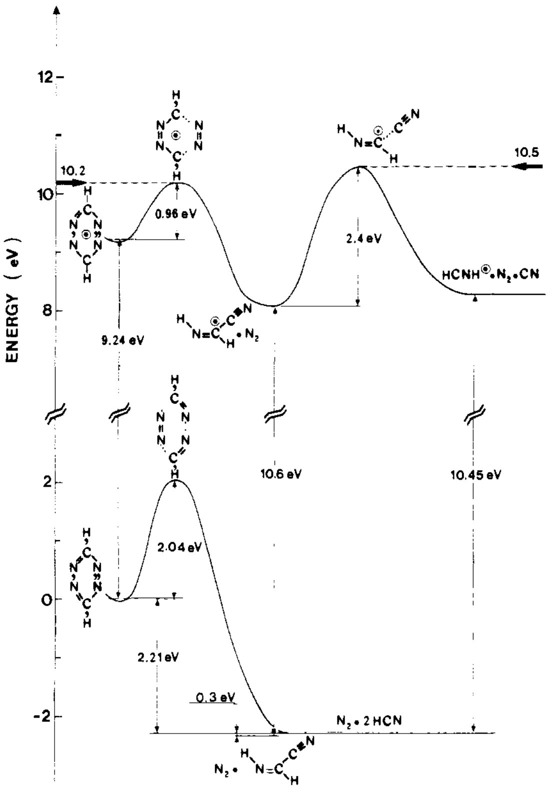

Figure 4. Thermochemistry diagram for the dissociation of the *s*-tetrazine ion into m/z 54 and 28. The structure of the $C_2N_2H_2^+$ fragment ion has been chosen arbitrarily to be that of isomer I (see text for details regarding the assumptions). The two arrows indicate the appearance energies of $C_2H_2N_2^+$ (10.2 eV) and $HCNH^+$ (10.5 eV).

From the breakdown curves of Figure 3, we have also extracted the appearance energies of major fragments, i.e., m/z 54, 28, 69, and 27. For others, such as m/z 30, 41, or 13, we have indicated the lowest photon energy for which the corresponding fragment has been observed. These values are reported in Table II together with heats of formation found in the literature.[20-22]

IV. Discussion

A. Structure of Fragment Ions. The determination of the structure of fragment is not straightforward because distinguishing N_2^+ from H_2CN^+ (m/z 28) or $C_2N_2H_2^+$ from CN_3^+ (m/z 54) requires isotope labeling. If these fragments have stable structures on the time scale of the observation (a few microseconds), we can safely eliminate CN_3^+. This ion (or the corresponding neutral) has not been observed to the best of our knowledge. In contrast, N_2^+ and H_2CN^+ have been found in ion–molecule reactions by Viggiano et al.[23] and in the dissociation of pyrazole and imidazole ions by Main-bobo et al.[24]

The structure of m/z 54 ($C_2N_2H_2^+$) requires consideration of several possible isomers. Experimental information is very scarce on this ion. A photoelectron study by Osman and Kroto[25] on (*Z*)-*c*-cyanoformimine N≡CCH=NH found the first IP to be at 10.6 eV. There is considerably more information available on the isomers of the neutral species. In Table III, we give the relative energies of the possible isomers of neutral $C_2N_2H_2$ as calculated by Clemmons et al.[12] relative to two isolated HCN molecules. These values are found to be satisfactory when compared with the available experimental observations reported in ref 12. Out of the seven isomers in Table III, there are only two forms that have significant stability compared to 2HCN, i.e., isomer I ((*Z*)-*c*-cyanoformimine) and isomer II, the linear van der Waals dimer HC≡N···HC≡N.

The ordering in energy for these isomers may be quite different in their ionic forms. Isomer VII can be eliminated because it cannot reasonably have an IP smaller than 9 eV. Isomer VI is a dissociation product and cannot account for the $C_2N_2H_2^+$ ions formation. Isomer III probably has an IP close to that of isomer I, i.e., ~10.6 eV; in both cases it corresponds to the ionization from a nitrogen electron lone pair in similar $C_2N_2H_2$ isomer structures. Isomers IV and V probably have a lower IP because it most probably corresponds to the ejection of a carbon electron lone pair. It has been shown by Jorgensen and Salem[27] that the IP of H—N=CH_2 (N lone pair ionization) is 11 eV, ~0.7 eV higher than the IP (10.34 eV) of C=N—CH_3 (C lone pair ionization). The case of isomer II, the HCN dimer, is more complicated. At a first glance, we would suppose that its IP is close to that of an isolated HCN molecule, i.e., 13.6 eV.[26] However, as the $HCN^+ + HCN \rightarrow H_2CN^+ + CN$ reaction is exothermic by ~2.2 eV, it probably rearranges very quickly in the more stable H_2CN^+···CN van der Waals ion, as it does in the case of the H_2O ionic dimers ($H_2O^+ \cdots H_2O \rightarrow H_3O^+ \cdots OH$). This effect would give an IP of ~11.1 eV for isomer II, the difference between the IP of HCN and the sum of the exothermicity of the above reaction plus the van der Waals bond energy (≈0.3 eV). In summary, the above considerations suggest a comparable stability to the I, II, III, IV, and V isomer structures of $C_2N_2H_2^+$, as reported in Table III.

The 11.2-eV spectrum (Figure 2) shows that m/z 53 and 52 fragments are as abundant as m/z 54. They are identified as $C_2N_2H^+$ and $C_2N_2^+$ ions. Their existence also supports the identification of m/z 54 as being $C_2N_2H_2^+$; the $C_2N_2^+H^+$ (m/z 53 ion) may result from the loss of H and may form an ion of the type N≡CCH=N^+. The $C_2N_2^+$ formation (in its well-known cyanogen form) requires either the loss of the H_2 from m/z 54 or the additional loss of an H atom from m/z 53. On energetic grounds, we suggest the loss of H_2 from $C_2N_2H_2^+$.

We now turn to the m/z 28 fragment that is prominent in our spectra. This fragment corresponds either to N_2^+ or $HCNH^+$. For comparison, we calculate the energy of the two limits $HCNH^+ + CN + N_2$ and $N_2^+ + 2HCN$, taking the ground state of neutral *s*-tetrazine at the origin of the potential energy. The $N_2 + 2HCN$ dissociation limit of neutral *s*-tetrazine has been estimated by Coulter et al.[2] to be −2.21 eV. The first N_2 IP is well-known[22] and is 15.58 eV. We readily obtain 13.37 eV for the thermodynamical limit $N_2^+ + 2HCN$. In contrast, the IP of HCNH is unknown. However, knowing that (i) the dissociation of HCN

---

[20] Cox, J. D.; Pilcher, G. *Thermochemistry of Organic and Organometallic Compounds*; Academic: New York, 1970.

[21] Federer, W.; Villinger, H.; Lindinger, W.; Ferguson, E. E. *Chem. Phys. Lett.* **1986**, *123*, 12.

[22] Rosenstock, H. M.; Draxl, K.; Steiner, B. W.; Herron, J. T. *J. Phys. Chem.* **1977**, *Ref. data 6*, Suppl. No. 1.

[23] Viggiano, A. F.; Howorka, F.; Albritton, D. L.; Fehsenfeld, F. C.; Adams, N. G.; Smith, D. *Astrophys. J.* **1980**, *236*, 492.

[24] Main-bobo, J.; Olesik, S.; Gase, W.; Bear, T.; Mommers, A. A.; Holmes, J. L. *J. Am. Chem. Soc.* **1986**, *108*, 677.

[25] Osman, O. I.; Kroto, H. W., private communication, 1987.

[26] Fridh, C.; Asbrink, L. *J. Electron Spectros. Rel. Phenom.* **1975**, *7*, 119.

[27] Jorgensen, W. L.; Salem, L. *The Organic Chemist's Book of Orbitals*; Academic: New York, 1973.

[28] Lias, S. G.; Libmann, J. F.; Levin, R. D. *J. Phys. Chem. Ref. Data* **1984**, *13*, 695.

Table III. $H_2C_2N_2$ and $H_2C_2N_2^+$ Isomers: Stabilities and First Ionization Potential (IP)

	$H_2C_2N_2$ isomers	calculated relative energy of neutral[a] kJ/mol	eV	IP (eV)	relative energy of ionic isomers with respect to ground-state neutral s-tetrazine[b] (eV)
Ia	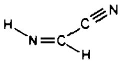	−29.8	−0.309	10.6[c]	8.08
Ib	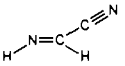	−29.1	−0.302	10.6[c]	8.088
II	$H{-}C{\equiv}N\cdots H{-}C{\equiv}N$	−26.3	−0.273	~11.1[d]	8.92
III	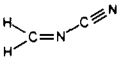	−2.8	−0.029	~10.6[d]	8.36
	$H{-}C{\equiv}N + H{-}C{\equiv}N$	0	0	13.6[e]	11.39
IVa	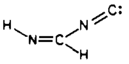	8.1	0.084	9.9 < IP < 10.6[d]	7.77 < *E* < 8.47
IVb	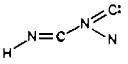	10.8	0.112	9.9 < IP < 10.6[d]	7.80 < *E* < 8.50
V	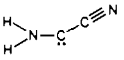	51.2	0.532	9.9 < IP < 10.6[d]	8.22 < *E* < 8.92
VI	$H_2 + N{\equiv}C{-}C{\equiv}N$	81.4	0.845	13.374 (C_2N_2) or 15.42 (H_2)[f]	12.00 or 14.05
VII	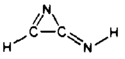	236.9	2.462	-	-

[a] Reference 12. 1 eV = 96.226 kJ/mol. [b] This value is calculated by taking the 2HCN energy at −2.21 eV with respect to ground state s-tetrazine. [c] Reference 25. [d] Estimation this work. [e] First IP from ref 26. [f] Reference 22.

into H + CN requires 4.3 eV,[20] (ii) the ionization potential of H is 13.6 eV, and (iii) the proton affinity of HCN is 7.45 eV,[27] we then conclude that this dissociation limit, $HCNH^+ + CN + N_2$, lies 10.45 eV above the N_2 + 2HCN one, and is therefore at 8.24 eV. Consequently, from the observation of *m/z* 28 below 13.37 eV photon energy we conclude that the *m/z* 28 is the $HCNH^+$ ion and not N_2^+.

The fragmentation pathways are summarized in Figure 4. We made use of the first adiabatic IP of *s*-tetrazine from the work of Fridh et al.,[8] the activation energy for triple dissociation of the neutral molecule,[5] and the determination of the relevant thermodynamical limits. Figure 4 also contains some information on the dissociation dynamics, which we shall address in the next section.

B. Dynamics of Dissociation. The appearance energies shown in Table II for *m/z* 54, 28, and 27 can be used to extract activation energies, only if the nature of the precursor is established. One important question here is this: does the *m/z* 28 ($HCNH^+$) originate from the parent ion in competition with the *m/z* 54 ($C_2N_2H_2^+$) production, or is it produced via a secondary event through the following sequence—*m/z* 82 → *m/z* 54 → *m/z* 28? From the abundance ratio of *m/z* 54 to *m/z* 28 (Figure 3) one observes that the latter appears at the expense of *m/z* 54. Either we are dealing with competing fragmentations and the rate for *m/z* 82 → *m/z* 28 is much larger than the rate for *m/z* 82 → *m/z* 54, or these dissociation processes are sequential and the *m/z* 54 abundance is ruled primarily by the *m/z* 28 appearance. In fact, we favor the sequential dissociation picture because of the following reasons.

In the competing fragmentation case, both the *m/z* 54 and 28 fragments are formed from the ground state of the ion. This means that both the lowest energy dissociation into two fragments and the somewhat higher energy dissociation into three fragments occur on the same electronic surface. The onset of *m/z* 54 is about 0.2 eV below that for *m/z* 28. Thus the rate of *m/z* 54 formation at the energy of the *m/z* 28 onset is already large. It is highly improbable, following conventional statistical theory, that the rate of triple dissociation should be faster than the lower energy *m/z* 54 formation. This contrasts the neutral molecule fragmentation case for which the lowest energy dissociation is to the three products.

The formation of *m/z* 28 ($HCNH^+$) clearly involves a rearrangement. This is inherently a slow reaction, probably slower than the loss of N_2 from the parent ion to form the *m/z* 54 fragment. The formation of $HCNH^+$ with its rearrangement is another contrast between the neutral and ionic reactions. In the neutral case, the formation of two HCN molecules with N_2 does not need any rearrangement.

Consequently, we suggest that the first step of the parent ion dissociation involves the breaking of two C–N bonds and the opening of the ring into a "quasilinear" fragment $HC{=}N{-}N{=}CH^+$, which is unstable and rearranges itself to a more stable form. The stable structure can be one of the isomer ions (I, II, III, IV, or V, discussed before). This ion then loses a CN molecule and produces $HCNH^+$. It also loses H to form *m/z* 53 and H_2 to form *m/z* 52. But, at this stage, in the absence of detailed information on the appearance energy of *m/z* 53 and 52, we cannot claim whether these hydrogen losses compete with the CN loss or not. It is interesting to note the difference between the dissociation of neutral *s*-tetrazine into three fragments (N_2 + 2HCN) and the dissociation of *s*-tetrazine ion into two fragments ($N_2 + C_2N_2H_2^+$). The stabilization of the $HC{=}N{-}N{=}CH^+$ intermediate, by the positive charge, is a key factor.

The reverse reactions exhibit large activation barriers (Figure 4) 2.11 eV for $C_2N_2H_2^+ + N_2 \rightarrow C_2N_4H_2^+$ and 2.26 eV for $HCNH^+ + CN \rightarrow C_2N_2H_2^+$. Such large reverse activation barriers suggest a large kinetic energy release in the dissociation. In the present case, we were unable to measure any broadening of the *m/z* 54 because of poor statistics and the presence of *m/z* 53 and 52 fragments. However, the broadening of *m/z* 28 can be observed at 11.2 eV. Notice that the loss of CN from $C_2N_2H_2^+$ leads to the breaking of a single bond into two fragments of almost equivalent masses. Therefore, the undectected CH fragment should carry away the same translational energy. The formation of *m/z* 54 favors the undetected N_2 fragment for carrying $^2/_3$ of the translational energy. The extent to which the reaction coordinate is coupled to the content of the fragment is not known at this point.

Finally, a few remarks regarding the formation of *m/z* 27 (HCN^+). This ion was found to appear at 11.4 eV, which is exactly the thermodynamical limit for $HCN^+ + HCN + N_2$ calculated from the first adiabatic IP of HCN.[26] Unlike the previous fragmentation processes, it is likely that the HCN^+ formation, which has no reverse activation barrier, probably is another m/z 54 dissociation channel with, of course, no kinetic energy release in the dissociation.

V. Conclusions

We have studied the photon selection of the *s*-tetrazine ion chemistry using synchrotron radiation in the 9–22 eV energy range. The *s*-tetrazine parent ion is found to dissociate at internal energies lower than the first excited state. This is reminiscent of the dissociation of the neutral molecule below the S_1 onset. In contrast to neutral *s*-tetrazine, the lowest parent ion dissociation path is to two fragments, $N_2 + C_2N_2H_2^+$, with an activation energy of 0.96 eV (at 10.2 eV photon energy). Calculations of relative stabilities of $C_2N_2H_2^+$ isomers would help in positively identifying the structure of this $C_2N_2H_2^+$ fragment. The loss of CN from $C_2N_2H_2^+$ is found to explain the further appearance of m/z 28 at 10.5 eV, which is identified as $HCNH^+$ and not N_2^+ (from thermochemistry). HCN^+ is found to appear at its thermodynamical limit around 11.4 eV. The overall fragmentation of *s*-tetrazine ion involves the formation of $N_2 + CN + HCNH^+$ via sequential dissociation steps (Figure 4). The nature of the process and products contrasts that of the neutral molecule case. This is probably because the large proton affinity of HCN favors the formation of $HCNH^+ + CN + N_2$ rather than $HCN + HCN^+ + N_2$ or $N_2^+ + 2HCN$, which requires higher internal energies.

Further investigation of the kinetic energy release and the rate constants of these dissociation pathways should provide further details of the steps involved, especially in cases where the reverse activation barriers are large. We plan further studies of the neutral fragmentation and ion kinetic energy distributions.

Acknowledgment. We thank M. Ait-Kaci for helping us take some of the data and M. C. Duval for suggestions regarding some critical steps in the *s*-tetrazine synthesis. We are indebted to C. Baudin and A. Ruaudel for providing us with *s*-tetrazine in large quantities (after a tedious and long procedure) and to H. Kroto for sending us his results prior to publications. Finally, we are grateful to T. Baer, P. Millie, E. Ferguson, C. Lifchitz, and P. Hiberty for useful discussions and suggestions and to the LURE staff for operating the ACO storage ring and the general facilities. One of us (A.H.Z.) thanks Professor J.-C. Lehmann for his hospitality at Ecole Normale Supêrieure and CNRS and the President's Fund at Caltech. The Guggenheim Foundation Fellowship is greatly appreciated for making this collaboration possible in France.

Registry No. Ia, 34892-77-8; Ib, 34892-76-7; II, 74-90-8; III, 43730-26-3; IVa, 85933-62-6; IVb, 85933-61-5; V, 1898-87-9; VI, 460-19-5; VII, 59559-12-5; $C_2N_4H_2$, 290-96-0; $C_2N_4H_2^+$, 105016-52-2.

Stereochemical Effects in the Gas-Phase Pinacol Rearrangement. 2. Ring Contraction versus Methyl Migration in *cis*- and *trans*-1,2-Dimethylcyclohexane-1,2-diol

Giulia de Petris,[†] Pierluigi Giacomello,*[†] Adriano Pizzabiocca,[‡] Gabriele Renzi,[‡] and Maurizio Speranza[‡]

Contribution from the Università di Roma "La Sapienza", 00185 Rome, Italy, and the Dipartimento di Scienze Chimiche, Università di Camerino, 62032 Macerata, Italy.
Received June 29, 1987

Abstract: The gas-phase pinacol rearrangement of *cis*- and *trans*-1,2-dimethylcyclohexane-1,2-diols, promoted by D_3^+, $CH_5^+/C_2H_5^+$ and t-$C_4H_9^+$ ions, was studied by mass spectrometric and radiolytic methods in the pressure range 0.5–760 Torr. When product isomerization is inhibited, by using $N(CH_3)_3$ as a trapping reagent at high pressure, mixtures of 2,2-dimethylcyclohexanone and 1-acetyl-1-methylcyclopentane were recovered from the reaction. In methane, the trend of the measured relative rates for ring contraction (k_5), methyl or hydroxyl group migration (k_6) versus the rearrangement rate of pinacol itself (k_p), is $k_6(trans) \simeq k_5(trans) \geq k_5(cis) > k_6(cis) \geq k_p$. No evidence for the formation of an intermediate carbenium ion was found. Stereochemical aspects of the mechanism are discussed and compared with solution data.

The combined application of mass spectrometric and radiolytic techniques was recently exploited to investigate the pinacol rearrangement of 1,2-dimethylcyclopentane-1,2-diols, promoted by gaseous Brønsted acids, and to show how the stereochemistry of the starting glycol influences the rate of the reaction.[1] In particular, methyl group participation in the rate-limiting loss of a water molecule was shown to take place in the cis epimer, which rearranges faster than the trans one to 2,2-dimethylcyclopentanone.

The study of the pinacol rearrangement in a gaseous environment allows one to follow the evolution of the protonated substrate along the reaction coordinate, in the absence of strong solvation interactions with the medium and competitive isomerization processes, thus displaying some stereochemical aspects which do not show up in solution experiments. This prompted us to extend the investigation to the rearrangement of 1,2-dimethylcyclohexane-1,2-diols (**1**), where the interplay of the stereochemistry of the reacting centers and the conformation of the substrates could help understanding the overall picture of the reaction mechanism.

The same reaction was studied in solution ($H_2O/HClO_4$),[2,3] where *cis*- and *trans*-**1** both gave some 2,2-dimethylcyclohexanone (**2**) together with predominant amounts of 1-acetyl-1-methylcyclopentane (**3**). The rearrangement is accompanied by isomerization of one diol to the other and ^{18}O exchange with the solvent. The data supported an A-1 mechanism and a common carbenium

---

[†] University of Roma.

[‡] University of Camerino.

(1) Part 1: de Petris, G.; Giacomello, P.; Picotti, T.; Pizzabiocca, A.; Renzi, G.; Speranza, M. *J. Am. Chem. Soc.* **1986**, *108*, 7491.

(2) (a) Nametkin, S.; Delectorsky, N. *Chem. Ber.* **1924**, *57*, 583. (b) Bartlett, P. D.; Pöckel, I. *J. Am. Chem. Soc.* **1937**, *59*, 820. (c) Meerwein, H. *Liebigs Ann. Chem.* **1939**, *542*, 123.

(3) Buton, C. A.; Carr, M. D. *J. Chem. Soc.* **1963**, 5854.

0002-7863/88/1510-1098$01.50/0